Ambegaokar-Baratoff relations for Josephson critical current in heterojunctions with multigap superconductors

Yukihiro Ota,[1,4] Noriyuki Nakai,[1,4] Hiroki Nakamura,[1,4,5] Masahiko Machida,[1,4,5] Daisuke Inotani,[2] Yoji Ohashi,[2,4] Tomio Koyama,[3,4] and Hideki Matsumoto[3,4]

[1]*CCSE, Japan Atomic Energy Agency, 6-9-3 Higashi-Ueno Taito-ku, Tokyo 110-0015, Japan*

[2]*Department of Physics, Keio University, 3-14-1 Hiyoshi, Kohoku-ku, Yokohama 223-8522, Japan*

[3]*Institute for Materials Research, Tohoku University, 2-1-1 Katahira Aoba-ku, Sendai 980-8577, Japan*

[4]*CREST(JST), 4-1-8 Honcho, Kawaguchi, Saitama 332-0012, Japan*

[5]*JST, TRIP, 5 Sambancho Chiyoda-ku, Tokyo 102-0075, Japan*

(Received 31 March 2010; revised manuscript received 21 May 2010; published 10 June 2010)

An extension of the Ambegaokar-Baratoff relation to a superconductor-insulator-superconductor (SIS) Josephson junction with multiple tunneling channels is derived. Applying the resultant relation to a SIS Josephson junction formed by an iron-based (five-band) and a single-band Bardeen-Cooper-Schrieffer (BCS) type superconductors, a theoretical bound of the Josephson critical current (I_c) multiplied by the resistance of the junction (R_n) is given. We reveal that such a bound is useful for identifying the pairing symmetry of iron-pnictide superconductors. One finds that if a measured value of I_cR_n is smaller than the bound then the symmetry is $\pm s$ wave, and otherwise s wave without any sign changes. In addition, we stress that temperature dependence of I_cR_n is sensitive to the difference of the gap functions from the BCS type gap formula in the above heterojunction.

DOI: 10.1103/PhysRevB.81.214511 PACS number(s): 74.50.+r, 74.70.Xa

I. INTRODUCTION

Since the discovery of iron-based superconductors,[1–7] their pairing symmetry has been intensively debated. According to the spin fluctuation mechanism associated with the Fermi surface nesting, $\pm s$-wave symmetry was proposed as a pairing scenario.[8–14] However, the debate has not been settled down. The $\pm s$-wave symmetry is expected to be fragile against nonmagnetic impurities.[15] Some experiment[16] supported this idea, while the others[17–21] presented controversial results. Hence, a direct and unambiguous evidence like the phase sensitive measurement in high-T_c cuprate superconductors[22] is now in great demand. In fact, a large number of the methods to seek a definite signature have been examined, e.g., tunneling spectroscopy,[23–27] corner junctions,[28–31] observation of half-integer flux-quantum jump,[32] scanning tunnel microscopy,[33] and so on.

Josephson junctions are sensitive devices reflecting superconducting states of each electrode. Very recently, various types of Josephson junctions with iron-pnictide superconductors were successfully fabricated and typical Josephson effects were confirmed.[34–37] Among them, a Josephson junction between an iron-based and a conventional s-wave single-gap superconductors has been regarded as a possible candidate to directly detect the pairing symmetry of iron-based superconductors. The heterojunction system is theoretically described by multiple tunneling channels, some of which are π channels and the others are 0 ones.[38,39] Authors suggested anomalous critical current reduction,[39] Riedel anomaly cancellation,[40] and enlargement of the Josephson vortex core.[41]

In this paper, we derive Ambagaokar-Baratoff relation[42] in the heterojunctions with multiple tunneling channels and clarify that a theoretical bound of I_cR_n products distinguishes $\pm s$-wave from s-wave without any sign changes, which is simply denoted as s wave throughout this paper. We examine two kinds of materials, $(Ba,K)Fe_2As_2$ (122 compound) and LaFeAs(O,F) (1111 compound) as the iron-based superconducting electrode in the heterojunction. Employing the density of states (DOS) ratios and the superconducting gap ratios given by five-band quasiclassical theory with the first-principles calculation,[43] the theoretical bounds are evaluated. The temperature dependences of I_cR_n are also demonstrated in both $\pm s$ wave and s wave.

The paper is organized as follows. Section II is the derivation of the Ambegaokar-Baratoff relation in the junction with multiple tunneling channels. Based on the result, we propose a criterion for identifying the pairing symmetry of iron-based superconductors. The key criterion is an upper bound of the Josephson critical current for the $\pm s$ wave, which corresponds to a lower bound for the s wave. In Sec. III, we apply this criterion to typical iron-pnictide superconducting materials and theoretically confirm its effectiveness. Section IV is devoted to the summary.

II. THEORETICAL BOUNDS OF JOSEPHSON CRITICAL CURRENTS

We examine a superconductor-insulator-superconductor (SIS) Josephson junction, as shown in Fig. 1. The electrode 1 (2), whose length is s' (s) in the direction of the z axis, is a single-band (five-band) superconductor. The insulator, whose length is d in the direction of the z axis and the dielectric constant is ϵ, is sandwiched between the two different superconducting electrodes.

One of the fundamental quantities characterizing Josephson junctions is the Josephson critical current density. One can find various discussion for the cases including two-band superconductors in several references.[25,39,44–46] However, there is no work on arbitrary N-band superconductors. This

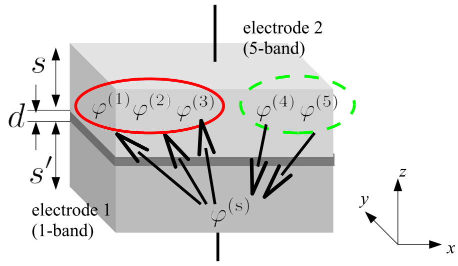

FIG. 1. (Color online) Schematic diagram of a SIS Josephson junction between five-band and single-band superconductors. Here the electrode 2 is assumed to be iron-based superconductor. The three superconducting phases enclosed by the solid line can be assigned as hole bands of iron-based superconductor, while the two phases enclosed by the dashed line as electron bands.

paper treats such a general case. Throughout this paper, we assume that there is no relative superconducting phase fluctuation in multiband superconducting electrodes. In this case, the system is described by an electric circuit as shown in Fig. 2. We remark that such a rigid parallel circuit modeling is a good description as far as the relative phase fluctuations are fully pinned. We will discuss corrections of relative phase fluctuations to Josephson effects elsewhere. Under this assumption, the total Josephson critical current density is given by

$$j_{\rm c} = \sum_i j_i \cos \chi_0^{(i1)}. \tag{1}$$

$\chi_0^{(ij)}$ is a constant phase between the ith and the jth superconducting gaps, which reflects the symmetry of a static gap solution. Equation (1) includes π channels when sign changes occur between the superconducting gaps. The basic formalism to derive Eq. (1) is shown in Appendix. For the s-wave case, $\chi_0^{(i1)}=0$ for any i. On the other hand, a part of $\{\chi_0^{(i1)}\}$ should be π for the $\pm s$-wave symmetry. As an example for the $\pm s$-wave case in the electrode 2, we take $\chi_0^{(21)}=\chi_0^{(31)}=\chi_0^{(32)}=0$ and $\chi_0^{(41)}=\chi_0^{(51)}=\pi$ as schematically shown in Fig. 2. Equation (1) indicates that $j_{\rm c}$ for the $\pm s$-wave symmetry is always smaller than that for the s wave, i.e., $j_{\rm c}(s \text{ wave}) > j_{\rm c}(\pm s \text{ wave})$.[39,46]

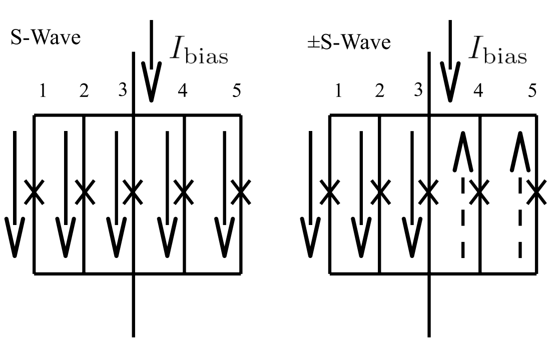

FIG. 2. Electric circuits corresponding to a SIS heterojunction. The circuit has the five parallel branches associated with the tunneling channels. The bias current is denoted as $I_{\rm bias}$. The left panel corresponds to the case of the s wave, while the right panel to the $\pm s$ wave.

Let us turn to a microscopic formula for j_i in Eq. (1). First, we give notations. As for the electrode 1, we denote the DOS on the Fermi surface and the superconducting gap amplitude as, respectively, $N_{\rm s}$ and $\Delta^{(\rm s)}$ (>0). Similarly, as for the electrode 2, N_i and $\Delta^{(i)}(>0)$ are the ith DOS and the ith gap amplitude, respectively. In addition, we define "smaller" and "larger" gaps as $\Delta_{{\rm S},i}=\min\{\Delta^{(i)},\Delta^{(\rm s)}\}$ and $\Delta_{{\rm L},i}=\max\{\Delta^{(i)},\Delta^{(\rm s)}\}$, respectively. Thus, assuming the full gap solutions in both superconducting electrodes, we microscopically calculate j_i using a standard second-order perturbation theory with respect to a tunneling channel.[42] Then, we have

$$j_i = \frac{1}{W}\frac{1}{r_{{\rm n},i}}\frac{\pi\Delta_{{\rm eff},i}}{2e},$$

where

$$\frac{1}{r_{{\rm n},i}} = \frac{4\pi e^2}{\hbar}|T^{(i)}|^2 N_{\rm s} N_i, \quad \Delta_{{\rm eff},i} = \frac{2}{\pi}K(k_i;\beta\Delta_{{\rm L},i})\Delta_{{\rm S},i},$$

and W is the area of the junction interface. In the definition of $r_{{\rm n},i}^{-1}$, the tunneling constant associated with the ith tunneling channel is denoted as $T^{(i)}$. The quantity k_i corresponds to the ratio of the smaller gap to the larger one, $k_i=[1-(\Delta_{{\rm S},i}/\Delta_{{\rm L},i})^2]^{1/2}$. The function $K(k;\nu)$ is given by

$$K(k;\nu) = \int_0^1 \frac{\tanh(\nu\sqrt{1-k^2x^2/2})}{\sqrt{(1-k^2x^2)(1-x^2)}}dx.$$

Combining the above arguments with Eq. (1), we obtain

$$I_{\rm c}R_{\rm n} = \sum_i \frac{R_{\rm n}}{r_{{\rm n},i}}\frac{\pi\Delta_{{\rm eff},i}}{2e}\cos \chi_0^{(i1)}, \tag{2}$$

where $I_{\rm c}=j_{\rm c}W$. The combined resistance $R_{\rm n}=1/\Sigma_i r_{{\rm n},i}^{-1}$ can be experimentally measured when a bias current is greater than $I_{\rm c}$, while the individual measurement of $r_{{\rm n},i}$ is practically impossible. Equation (2) is a generalized formula of the Ambegaokar-Baratoff relation for multichannel heterojunctions. Brinkman *et al.*[44] and Agterberg *et al.*[45] obtained similar results in the context of MgB_2, i.e., two-band superconductor.

Here, we derive a simple relation from Eq. (2) when the electrode 2 has the s-wave symmetry. The resultant expression can give useful information about the pairing symmetry. The right-hand side of Eq. (2) is a summation of positive quantities in this case (i.e., $\chi_0^{(i1)}=0$ for any i). Accordingly, we find that

$$I_{\rm c}(s\text{-wave})R_{\rm n} \geq \frac{\pi\Delta_*}{2e}, \quad \Delta_* = \min_i \Delta_{{\rm eff},i}, \tag{3}$$

which gives a theoretical lower bound of $I_{\rm c}R_{\rm n}$ for the s wave. From the above argument, we find that if the symmetry of the electrode 2 is s wave then Eq. (3) must be fulfilled. Namely, if a measured value of $I_{\rm c}R_{\rm n}$ satisfies the inequality

$$I_{\rm c}R_{\rm n} < \frac{\pi\Delta_*}{2e}, \tag{4}$$

then one can exclude the possibility of the s wave. This method does not give more detailed information about the

TABLE I. DOS ratios on the Fermi surfaces of iron-based materials evaluated by a first-principles calculation (Ref. 43). The first three DOS's (N_1, N_2, and N_3) corresponds to the hole bands, while the remaining DOS's (N_4 and N_5) to the electric bands.

	N_1/N_{tot}	N_2/N_{tot}	N_3/N_{tot}	N_4/N_{tot}	N_5/N_{tot}
$BaFe_2As_2$	0.1687	0.2757	0.2104	0.1803	0.1649
LaFeAsO	0.1133	0.3009	0.2323	0.1608	0.1928

symmetry but clarify whether π channels exist in the multiple tunneling junctions with iron-pnictides. The present scheme, "lower-bound criterion" is a simple and convenient classification of iron-based superconducting materials.

Let us discuss experimental applicability of the criterion. The direct experimental data for bulk superconducting samples, e.g., angle resolved photoemission spectroscopy,[47,48] provides the gap amplitudes in the one-gap and the iron-based superconducting electrodes. Therefore, in principle, one can input Δ_* in Eq. (3). However, superconducting gap amplitudes relevant to Josephson junctions is generally smaller than the ones in the bulk superconductors due to the damage piled up in interface fabrication. It indicates that direct comparison of a measured I_cR_n product to Δ_* based on the bulk data may give no practical information. Therefore, we focus on a transition voltage of the all tunneling channels into running state at zero temperature,[49]

$$V_0 = \frac{1}{e}[\Delta^{(s)}(T=0) + \Delta_{max}(T=0)], \tag{5}$$

in which $\Delta_{max} = \max_i \Delta^{(i)}$. One can measure the suppressed V_0 experimentally if the junction shows hysteretic *I-V* characteristics.[49] We emphasize that a scaled quantity Δ_*/eV_0 is given by only the gap amplitude ratios since the bulk gap ratios are expected to be kept as long as the damage is not too severe. Therefore, the scaled lower bound Δ_*/eV_0 is experimentally evaluated by the gap amplitude ratios for the bulk samples, and this quantity should be compared to measured I_cR_n/V_0. Consequently, we conclude that the inequality [Eq. (4)] is an effective formula to examine the pairing symmetry.

III. APPLICATION OF LOWER-BOUND CRITERION TO IRON-PNICTIDE SUPERCONDUCTORS

Let us evaluate the right-hand side of Eq. (2) in real iron-pnictide materials and check how the criterion based on the inequality [Eq. (4)] works. For the sake of simplicity, we employ a simple model for the tunneling constants. Namely, we assume that $T^{(i)}$'s take channel-independent constants. It means that $R_n/r_{n,i}$ is equal to N_i/N_{tot}, where $N_{tot} = \Sigma_i N_i$. Then, we find that I_cR_n/V_0 is simply a function of the superconducting gap ratios (i.e., $\Delta^{(s)}/\Delta_{max}$ and $\Delta^{(i)}/\Delta_{max}$) and the DOS ratios (i.e., N_i/N_{tot}).

We concentrate on two iron-pnictide superconducting materials, $(Ba,K)Fe_2As_2$ ($T_c^{122}=38$ K) and LaFeAs(O,F) ($T_c^{1111}=27$ K). Here, we denote each superconducting transition temperature as T_c^{122} or T_c^{1111}. As for the single-gap superconducting electrode material, we choose an alloy of Pb, i.e., Pb-In-Au. The superconducting transition temperature $T_c^{s}=7$ K and $\Delta^{(s)}(0)/k_BT_c^{s}=1.98$, respectively.[50] The gap amplitude ratios and their temperature dependence of $(Ba,K)Fe_2As_2$ and LaFeAs(O,F) were evaluated by five-band quasiclassical theory combined with the DOS's via the first-principles calculations and several kinds of experimental data for the bulk properties.[43] We label three hole bands as 1 to 3 and two electron ones as 4 to 5. The sign changes are assumed to occur between the hole and the electron bands. The DOS and the gap ratios are summarized in Tables I and II, respectively. As for the temperature dependence of the single-band superconducting gap, we utilize the BCS type gap formula[51]

$$\Delta^{(s)}(T) = \Delta^{(s)}(0)\tanh\left\{A\left[B\left(\frac{T_c^{s}}{T}-1\right)\right]^{C}\right\}, \tag{6}$$

where $A=1.82$, $B=1.018$, and $C=0.51$.

Figure 3 displays the temperature dependence of the superconducting gap amplitudes. Figure 4 shows the temperature dependence of I_cR_n normalized by V_0. The lower bound at $T=0$ given by the right hand side of the inequality [Eq. (3)] is also depicted by the (blue) horizontal line. Due to $j_c(s \text{ wave}) > j_c(\pm s \text{ wave})$, I_cR_n for the $\pm s$ wave becomes smaller than the one for the s wave over all temperature regions. Here, let us focus on the zero temperature. I_cR_n/V_0 for the $\pm s$ wave is smaller than the lower bound $[\pi\Delta_*(0)/2eV_0]$ while that for s wave is larger for both of the iron-pnictide superconducting materials. Hence, the comparison of a measured value of I_cR_n to the theoretical bound gives a useful criterion for the symmetry in the iron-based superconductors.

TABLE II. Superconducting gap amplitude ratios of iron-pnictide materials at zero temperature estimated by a five-band quasiclassical theory (Ref. 43).

($T=0$ K)	$\Delta^{(1)}/\Delta_{max}$	$\Delta^{(2)}/\Delta_{max}$	$\Delta^{(3)}/\Delta_{max}$	$\Delta^{(4)}/\Delta_{max}$	$\Delta^{(5)}/\Delta_{max}$	$2\Delta_{max}/k_BT_c^{iron}$	$\Delta^{(s)}/\Delta_{max}$
$(Ba,K)Fe_2As_2$	0.9395	1	0.5189	0.9415	0.9691	3.785	0.192
LaFeAs(O,F)	0.5052	1	0.2677	0.5084	0.5300	4.426	0.232

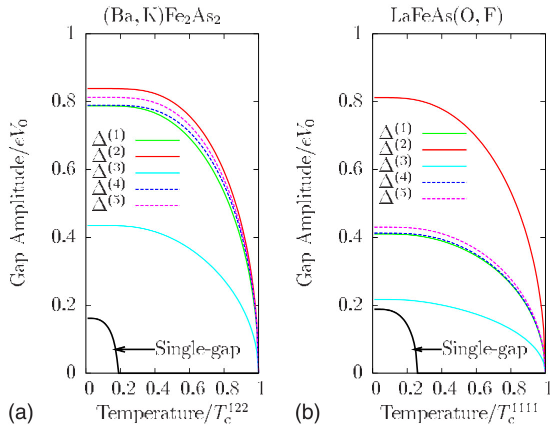

FIG. 3. (Color online) Temperature dependence of iron-pnictide and single-band superconductor gap amplitudes. As for the iron-pnictide materials, we employ the previous results (Ref. 43). The gap amplitudes are normalized by $eV_0=e[\Delta^{(s)}(0)+\Delta_{\max}(0)]$. The solid lines ($\Delta^{(1)}$, $\Delta^{(2)}$, and $\Delta^{(3)}$) correspond to the hole band, while the dashed lines ($\Delta^{(4)}$ and $\Delta^{(5)}$) the electric band. In the case of the $\pm s$-wave symmetry, the gaps corresponding to the dashed lines have the relative minus signs (i.e., $\chi_0^{(41)}=\chi_0^{(51)}=\pi$). (a) $(Ba,K)Fe_2As_2$ ($T_c^{122}=38$ K) and (b) LaFeAs(O,F) ($T_c^{1111}=27$ K).

Next, we investigate specific cases in which a part of or all iron-based superconducting gaps are smaller than the single-band BCS gap, as shown in Figs. 5(a) and 5(b). In such a study, we keep the gap ratios to be the values for $(Ba,K)Fe_2As_2$ shown in Tables I and II except for $\Delta^{(s)}/\Delta_{\max}$. Figures 5(c) and 5(d) show the I_cR_n's for $T_c^{122}=10$ and 6 K, respectively. We find again that the inequality [Eq. (4)] is fulfilled at zero temperature. It means that the present criterion works in every case. On the other hand, we notice that the temperature dependences of I_cR_n are relatively anomalous. We find a convex behavior in the middle temperature range (i.e., $T/T_c^{122}\sim0.2-0.8$) contrary to our naive expectation. Such peculiarity comes from a discrepancy between the gap functions calculated by the five-band quasiclassical theory and the BCS type gap formula (6), as shown in Fig. 6. In the previous case as Fig. 4, the single-band BCS gap solely provides the contributions to the temperature dependence of I_cR_n. However, the present case reflects all the gap temperature dependences. Thus, the temperature dependence of I_cR_n is found to be quite sensitive to the difference of the gap functions from the single-band BCS type gap formula.[52]

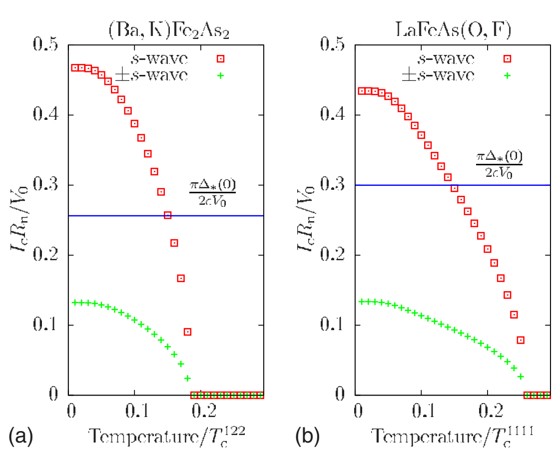

FIG. 4. (Color online) I_cR_n products normalized by Eq. (5). The red squares are for the s-wave, while the green crosses are for the $\pm s$-wave symmetry (i.e., $\chi_0^{(21)}=\chi_0^{(31)}=0$ and $\chi_0^{(41)}=\chi_0^{(51)}=\pi$). We also show the theoretical lower bounds for the s-wave symmetry at zero temperature ($\pi\Delta_*(0)/2eV_0$), depicted as the blue solid lines. We find that I_cR_n/V_0 for $\pm s$ wave is much smaller than the theoretical lower bound for the s-wave at zero temperature. (a) $(Ba,K)Fe_2As_2$ ($T_c^{122}=38$ K) and (b) LaFeAs(O,F) ($T_c^{1111}=27$ K).

IV. SUMMARY

We derived the Ambegaokar-Baratoff relation in the SIS Josephson junction with multiple (more than two) tunneling channels and proposed a criterion to identify the pairing symmetry of the iron-based superconductors. If a measured value of I_cR_n product is smaller than the lower bound for the s wave, then one concludes that the symmetry of the superconducting electrode is the $\pm s$ wave. We actually revealed that the criterion well works in the typical iron-pnictide superconductors by employing the DOS and the gap ratios calculated by the five-band quasiclassical theory and the first-principles calculation. In addition, the theory predicted that the temperature dependence of I_cR_n is sensitive to the deviation of the temperature dependence of the gap from the single-band BCS formula. The method is simple and convenient in contrast to the phase sensitive measurement like π junctions which require much more elaborate setups.

The Ambegaokar-Baratoff relation is one of the fundamental identity in the SIS Josephson junction. The present analysis suggested that this type of the relation provides more fruitful information when the junction has multiple tunneling channels.

ACKNOWLEDGMENTS

The authors (Y.O. and M.M.) wish to acknowledge valuable discussion with S. Shamoto, N. Hayashi, Y. Nagai, M. Okumura, and R. Igarashi. They also would like to thank I. Kakeya for helpful comments. The work was partially supported by Grant-in-Aid for Scientific Research on Priority Area "Physics of new quantum phases in superclean materials" (Grant No. 20029019) from the Ministry of Education, Culture, Sports, Science and Technology of Japan.

APPENDIX: FORMALISM FOR GAUGE-INVARIANT PHASE DIFFERENCES

A basic formalism for the hetero Josephson junction dealt in this paper is presented. Assuming uniformity along y axis, the effective Lagrangian density on the zx plane[39] is given by

$$\mathcal{L}_{\text{eff}}=\frac{s'}{8\pi\mu'^2}(q^0)^2+\sum_{i=1}^{5}\frac{s}{8\pi\mu_i^2}(q_i^0)^2+\sum_{i=1}^{5}\frac{\hbar j_i}{e^*}\cos\theta^{(i)}+\sum_{i<i'}\frac{\hbar J_{ii'}}{e^*}\cos\chi^{(i'i)}+\frac{d\epsilon}{8\pi}(E_{21}^z)^2, \tag{A1}$$

where $\theta^{(i)}=\varphi^{(i)}-\varphi^{(s)}(e^*d/\hbar c)A_{21}^z$ and $\chi^{(i'i)}=\varphi^{(i')}-\varphi^{(i)}=\theta^{(i')}$

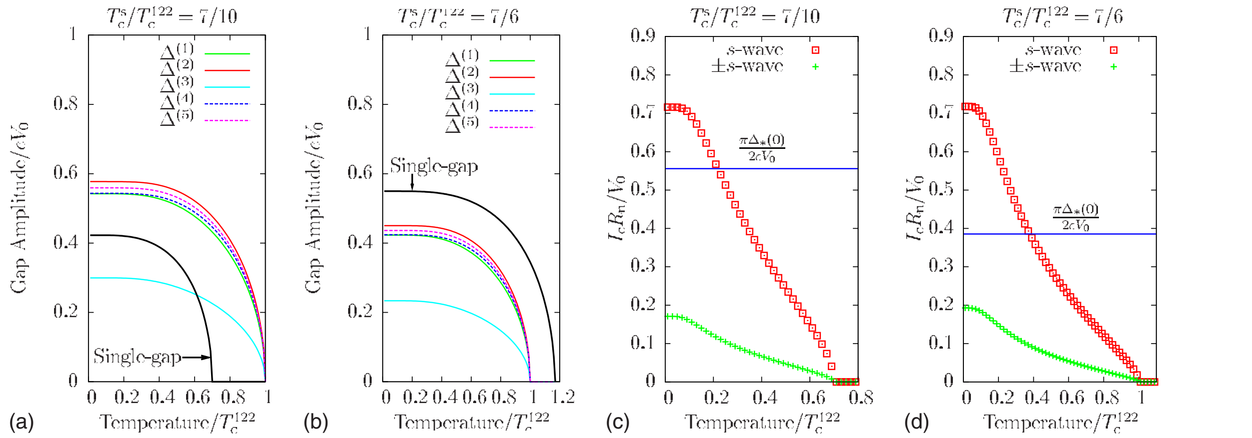

FIG. 5. (Color online) Results for smaller iron-pnictide superconducting gap amplitudes. The DOS and the gap ratios are the same as the ones in Fig. 4(a), but the iron-pnictide superconducting transition temperatures are much smaller than in the previous example. The I_cR_n products normalized by Eq. (5) are shown in (c) [(d)], in which the gap amplitudes drawn in (a) [(b)] are employed.

$-\theta^{(i)}$. $\chi^{(i'i)}$ is the relative phase difference between the different superconducting gaps. The first and the second terms in Eq. (A1) represent charge compressibility in the electrode 1 and 2, respectively, where $q^0=(\hbar/e^*)\partial_t\varphi^{(s)}+A_1^0$, $a_i^0=(\hbar/e^*)\partial_t\varphi^{(i)}+A_2^0$, and $e^*=2e$. The electric scalar potential in the electrode $\ell(=1,2)$ is denoted as A_ℓ^0, and the charge screening length in the electrode 1 (2) is written as μ' (μ_i). The third term in Eq. (A1) is the Josephson coupling, in which $\hbar j_i/e^*$ is the coupling constant associated with the ith tunneling channel. The forth term in Eq. (A1) is called the interband Josephson coupling energy,[53] whose origin is the interband interaction between different bands in the electrode 2. In the gauge-invariant phase difference $\theta^{(i)}$, the vector potential in the insulator $A_{21}^z=d^{-1}\int_{-d/2}^{d/2}A^z(z)dz$, in which $A^z(z)$ is the z component of the vector potential. The electric field is expressed as $E_{21}^z=-c^{-1}\partial_t A_{21}^z-d^{-1}(A_2^0-A_1^0)$.

As the Euler-Lagrangian equation with respect to A_ℓ^0, we obtain the Josephson relation

$$\sum_i \frac{\bar{\alpha}}{\alpha_i}\partial_t\theta^{(i)}=\frac{e^*\Lambda d}{\hbar}E_{21}^z, \tag{A2}$$

where $\alpha'=\epsilon\mu'^2/s'd$, $\alpha_i=\epsilon\mu_i^2/sd$, $\bar{\alpha}^{-1}=\Sigma_i\alpha_i^{-1}$, and $\Lambda=1+\alpha'+\bar{\alpha}$. Next, as the Euler-Lagrangian equation with respect to A_{21}^z, we have the Maxwell equation

$$0=\frac{\epsilon}{c^2}\frac{e^*d}{\hbar}\partial_t E_{21}^z+\sum_i\frac{4\pi e^*d}{\hbar c^2}j_i\sin\theta^{(i)}. \tag{A3}$$

Combining Eq. (A3) with Eq. (A2) leads to the equation

$$\frac{\epsilon}{4\pi\Lambda d}\frac{\hbar}{e^*}\sum_i\frac{\bar{\alpha}}{\alpha_i}\partial_t^2\theta^{(i)}+\sum_i j_i\sin\theta^{(i)}=0. \tag{A4}$$

If one adds a dissipation and an external bias current terms to Eq. (A4), one has the resistively and capacitively shunted junction model with multitunneling channels.

Let us turn to a formula for the Josephson critical current density. Generally, the system has a relative superconducting phase fluctuation originating from the interband Josephson coupling $\Sigma_{i<i'}J_{ii'}\cos\chi^{(i'i)}$, which generates Josephson-Leggett collective excitation modes.[39,53] The equations of motion for $\chi^{(i'i)}$ can be obtained as the Euler-Lagrange equations with respect to $\varphi^{(s)}$ and $\varphi^{(i)}$.[39] In this paper, we simply assume that each $\chi^{(i'i)}$ is fixed as a constant $\chi_0^{(i'i)}$ reflecting the symmetry of a static gap solution. Such an assumption can be validated when $|J_{ii'}|\gg j_1,j_2$. In this case, we have $\theta^{(i)}(t)=\theta^{(1)}(t)+\chi_0^{(i1)}$, where $\chi_0^{(i1)}=0$ or π. Equation (A4) is then rewritten by

$$\frac{\epsilon}{4\pi\Lambda d}\frac{\hbar}{e^*}\partial_t^2\theta^{(1)}+\sum_i j_i\cos\chi_0^{(i1)}\sin\theta^{(1)}=j_{\mathrm{bias}}. \tag{A5}$$

Here, we add a bias current density j_{bias} to the right-hand side. Equation (A5) indicates that a static solution exists as long as $j_{\mathrm{bias}}<|\Sigma_i j_i\cos\chi_0^{(i1)}|$.

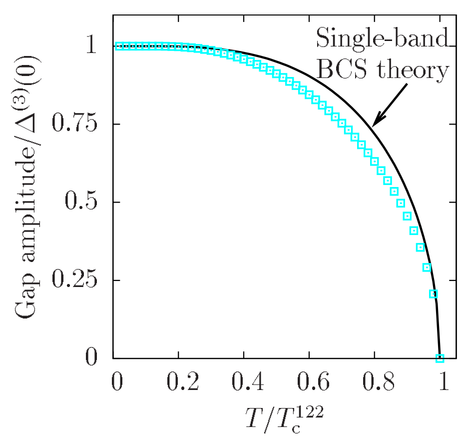

FIG. 6. (Color online) Comparison of iron-pnictide's gap function to the single-band BCS gap function. The cyan square is the small gap $\Delta^{(3)}$ calculated by the five-band quasiclassical theory for (Ba,K)Fe_2As_2 (Ref. 43), while the black solid line corresponds to Eq. (6), in which we use T_c^{122} instead of T_c^s. One finds that a difference between the two functions exists around $T/T_c^{122}=0.4$–0.8. We can find a similar discrepancy for $\Delta^{(1)}$, which is much smaller than in the present figure.

[1] Y. Kamihara, T. Watanabe, M. Hirano, and H. Hosono, J. Am. Chem. Soc. **130**, 3296 (2008).
[2] Ren Zhi-An, Lu Wei, Yang Jie, Yi Wei, Shen Xiao-Li, Zheng-Cai, Che Guang-Can, Dong Xiao-Li, Sun Li-Ling, Zhou Fang, and Zhao Zhong-Xian, Chin. Phys. Lett. **25**, 2215 (2008).
[3] M. Rotter, M. Tegel, and D. Johrendt, Phys. Rev. Lett. **101**, 107006 (2008).
[4] K. Sasmal, B. Lv, B. Lorenz, A. M. Guloy, F. Chen, Y.-Y. Xue, and C.-W. Chu, Phys. Rev. Lett. **101**, 107007 (2008).
[5] J. H. Tapp, Z. Tang, B. Lv, K. Sasmal, B. Lorenz, P. C. W. Chu, and A. M. Guloy, Phys. Rev. B **78**, 060505(R) (2008).
[6] X. C. Wang, Q. Liu, Y. Lv, W. Gao, L. X. Yang, R. C. Yu, F. Y. Li, and C. Jin, Solid State Commun. **148**, 538 (2008).
[7] F.-C. Hsu, J.-Y. Luo, K.-W. Yeh, T.-K. Chen, T.-W. Huang, P. M. Wu, Y.-C. Lee, Y.-L. Huang, Y.-Y. Chu, D.-C. Yan, and M.-K. Wu, Proc. Natl. Acad. Sci. U.S.A. **105**, 14262 (2008).
[8] I. I. Mazin, D. J. Singh, M. D. Johannes, and M. H. Du, Phys. Rev. Lett. **101**, 057003 (2008).
[9] K. Kuroki, S. Onari, R. Arita, H. Usui, Y. Tanaka, H. Kontani, and H. Aoki, Phys. Rev. Lett. **101**, 087004 (2008); **102**, 109902(E) (2009).
[10] S. Graser, T. A. Maier, P. J. Hirschfeld, and D. J. Scalapino, New J. Phys. **11**, 025016 (2009).
[11] F. Wang, H. Zhai, Y. Ran, A. Vishwanath, and D.-H. Lee, Phys. Rev. Lett. **102**, 047005 (2009).
[12] S.-L. Yu, J. Kang, and J.-X. Li, Phys. Rev. B **79**, 064517 (2009).
[13] V. Cvetkovic and Z. Tesanovic, EPL **85**, 37002 (2009).
[14] K. Kuroki, H. Usui, S. Onari, R. Arita, and H. Aoki, Phys. Rev. B **79**, 224511 (2009).
[15] S. Onari and H. Kontani, Phys. Rev. Lett. **103**, 177001 (2009).
[16] Y. F. Guo, Y. G. Shi, S. Yu, A. A. Belik, Y. Matsushita, M. Tanaka, Y. Katsuya, K. Kobayashi, I. Nowik, I. Felner, V. P. S. Awana, K. Yamaura, and E. Takayama-Muromachi, arXiv:0911.2975 (unpublished).
[17] S. C. Lee, A. Kawabata, T. Moyoshi, Y. Kobayashi, and M. Sato, J. Phys. Soc. Jpn. **78**, 043703 (2009).
[18] Y. Li, X. Lin, Q. Tao, C. Wang, T. Zhou, L. Li, Q. Wang, M. He, G. Cao, and Zhu'an Xu, New J. Phys. **11**, 053008 (2009).
[19] M. Sato, Y. Kobayashi, S. C. Lee, H. Takahashi, E. Satomi, and Y. Miura, J. Phys. Soc. Jpn. **79**, 014710 (2010).
[20] P. Cheng, B. Shen, J. Hu, and H.-H. Wen, Phys. Rev. B **81**, 174529 (2010).
[21] Y. Li, J. Tong, Q. Tao, C. Feng, G. Cao, Zhu-an Xu, W. Chen, and F.-C. Zhang, arXiv:1001.4317 (unpublished).
[22] C. C. Tsuei and J. R. Kirtley, Rev. Mod. Phys. **72**, 969 (2000).
[23] S. Onari and Y. Tanaka, Phys. Rev. B **79**, 174526 (2009).
[24] J. Linder and A. Sudbø, Phys. Rev. B **79**, 020501(R) (2009).
[25] I. B. Sperstad, J. Linder, and A. Sudbø, Phys. Rev. B **80**, 144507 (2009).
[26] Y. Nagai and N. Hayashi, Phys. Rev. B **79**, 224508 (2009).
[27] A. A. Golubov, A. Brinkman, Y. Tanaka, I. I. Mazin, and O. V. Dolgov, Phys. Rev. Lett. **103**, 077003 (2009).
[28] W.-F. Tsai, D.-X. Yao, B. A. Bernevig, and J. P. Hu, Phys. Rev. B **80**, 012511 (2009).
[29] D. Parker and I. I. Mazin, Phys. Rev. Lett. **102**, 227007 (2009).
[30] J. S. Wu and P. Phillips, Phys. Rev. B **79**, 092502 (2009).
[31] W.-Q. Chen, F. Ma, Z.-Y. Lu, and F.-C. Zhang, Phys. Rev. Lett. **103**, 207001 (2009).
[32] C.-T. Chen, C. C. Tsuei, M. B. Ketchen, Z.-A. Ren, and Z. X. Zhao, Nat. Phys. **6**, 260 (2010).
[33] T. Hanaguri, S. Niitaka, K. Kuroki, and H. Takagi, Science **328**, 474 (2010).
[34] X. Zhang, Y. S. Oh, Y. Liu, L. Yan, K. H. Kim, R. L. Greene, and I. Takeuchi, Phys. Rev. Lett. **102**, 147002 (2009).
[35] X. Zhang, S. R. Saha, N. P. Butch, K. Kirshenbaum, J. Paglione, R. L. Greene, Y. Liu, L. Yan, Y. S. Oh, K. H. Kim, and I. Takeuchi, Appl. Phys. Lett. **95**, 062510 (2009).
[36] H. Kashiwaya, K. Shirai, T. Matsumoto, H. Shibata, H. Kambara, M. Ichikado, H. Eisaki, A. Iyo, S. Shamoto, I. Kurosawa, and S. Kashiwaya, Appl. Phys. Lett. **96**, 202504 (2010)..
[37] T. Katase, Y. Ichimaru, A. Tsukamoto, H. Hiramatsu, T. Kamiya, K. Tanabe, and H. Hosono, Appl. Phys. Lett. **96**, 142507 (2010).
[38] J. Linder, I. B. Sperstad, and A. Sudbø, Phys. Rev. B **80**, 020503(R) (2009).
[39] Y. Ota, M. Machida, T. Koyama, and H. Matsumoto, Phys. Rev. Lett. **102**, 237003 (2009).
[40] D. Inotani and Y. Ohashi, Phys. Rev. B **79**, 224527 (2009).
[41] Y. Ota, M. Machida, T. Koyama, and H. Matsumoto, Phys. Rev. B **81**, 014502 (2010).
[42] V. Ambegaokar and A. Baratoff, Phys. Rev. Lett. **10**, 486 (1963); **11**, 104 (1963).
[43] N. Nakai, H. Nakamura, Y. Ota, Y. Nagai, N. Hayashi, and M. Machida, arXiv:0909.1195 (unpublished).
[44] A. Brinkman, A. A. Golubov, H. Rogalla, O. V. Dolgov, J. Kortus, Y. Kong, O. Jepsen, and O. K. Andersen, Phys. Rev. B **65**, 180517(R) (2002).
[45] D. F. Agterberg, E. Demler, and B. Janko, Phys. Rev. B **66**, 214507 (2002).
[46] Y. Ota, M. Machida, and T. Koyama, J. Phys. Soc. Jpn. **78**, 103701 (2009).
[47] H. Ding, P. Richard, K. Nakayama, K. Sugawara, T. Arakane, Y. Sekiba, A. Takayama, S. Souma, T. Sato, T. Takahashi, Z. Wang, X. Dai, Z. Fang, G. F. Chen, J. L. Luo, and N. L. Wang, EPL **83**, 47001 (2008).
[48] D. V. Evtushinsky, D. S. Inosov, V. B. Zabolotnyy, M. S. Viazovska, R. Khasanov, A. Amato, H.-H. Klauss, H. Luetkens, Ch. Niedermayer, G. L. Sun, V. Hinkov, C. T. Lin, A. Varykhalov, A. Koitzsch, M. Knupfer, B. Büchner, A. A. Kordyuk, and S. V. Borisenko, New J. Phys. **11**, 055069 (2009).
[49] V. V. Schmidt, *The Physics of Superconductors: Introduction to Fundamentals and Applications* (Springer-Verlag, Berlin, 1997), Chap. 6.
[50] J. H. Hinken, *Superconductor Electronics: Fundamentals and Microwave Applications* (Springer-Verlag, Berlin, 1991), Chap. 5.
[51] A. Carrington and F. Manzano, Physica C **385**, 205 (2003).
[52] As pointed out by Sperstad *et al.* (Ref. 25), the contribution from the Andreev reflection can bring about another peculiar behavior in the temperature dependence of I_c, i.e., a sharp peak near T_c when the single-band gap crosses iron-pnictide's gaps as shown in Fig. 5(a).
[53] A. J. Leggett, Prog. Theor. Phys. **36**, 901 (1966).